

Evaluating Land Degradation Vulnerability Using Analytical Hierarchy Process (AHP) And Geo-Spatial Techniques In The Mashi Dam Command Area, Rajasthan (India)

Brijmohan Bairwa^{1*}, Rashmi Sharma²

^{1&2} School of Earth Sciences, Banasthali Vidyapith, Rajasthan, India

Abstract: - Land degradation stands as a primary environmental calamity caused by combination of human activities and natural factors, affecting the sustainability of soil and ecosystems in arid and semi-arid regions globally. This issue underscores the necessity for identifying and planning vulnerability zones of land degradation at various scales, ranging from regional to micro levels. In this research work, rainfall, potential evapotranspiration (PET), data were extracted from Terra climate, while land surface temperature (LST) were extracted from Landsat series using the Climate Engine platform. Additionally, the study incorporated land-use/land-cover (LULC) information derived from Sentinel-2A imagery, as well as data on drainage and canal systems, elevation, slope, and key soil properties like electrical conductivity (EC) and exchangeable sodium percentage (ESP). Among these parameters, EC, ESP, LULC, PET and canal system were determined to be the most significant factors, followed by elevation, slope, LST, drainage and precipitation. Geospatial techniques derived products, and the analytical hierarchy process (AHP) were employed to model the land degradation vulnerability index (LDVI). The LDVI was classified into three classes: highly vulnerable (7.63%), moderately vulnerable (52.12%), and slightly vulnerable (40.26%) to viewing the affected fields due to the land degradation factors. The typically western part of the main canal of the study area, characterized by low precipitation rates vulnerable to evaporation under high temperatures, was identified as highly vulnerable to land degradation (LD), while the eastern part of the study area exhibited the opposite trend. The model's applicability was validated using high resolution dataset (Google Earth), demonstrating its effectiveness in the study. Furthermore, the validation using the Receiver Operating Characteristic (ROC) curve analysis yielded an area under curve (AUC) value of 80.6%, affirming the AHP method's accuracy in predicting LD vulnerability fields in the study area. This study significantly contributes to understanding the impact of land degradation on sustainable agriculture management and development in the Mashi Dam Command Area (MDCA), Rajasthan (India).

Keywords: Soil Degradation, Vulnerability study, Multi Criteria Decision Analysis, Geo-Informatics, Rajasthan (India).

1. Introduction

Land and soil play a vital role in regulating biodiversity, providing essential ecosystem services, and contributing to global biogeochemical cycles. It is responsible for carbon sequestration, nutrient cycling, water filtration, and the provision of habitats for diverse species. Land eco-systems also contribute to the overall stability and resilience of the planet's biosphere (Smith, P., et al. 2013). However, the aforementioned pressures, such as soil erosion, land degradation, deforestation, habitat loss, soil pollution, and climate change have significant impacts on ecosystem functioning. They contribute to the decline of species populations and disrupt the delivery of important ecosystem services. Studies conducted by Morgado et al. (2018) and Costantini et al. (2009) provide evidence of the detrimental effects of these pressures on ecosystems and their ability to provide vital services to humanity.

Land degradation is a pressing issue, particularly developing countries as well as arid and semi-arid regions at the global level. Land degradation has direct implications for food security, human well-being, and development (Gomiero, 2016; Hossain et al., 2020; Crossland et al., 2018; Gichenje et al., 2019). It can be described as a

To address land degradation, it is essential to consider climate parameters (precipitation, and evapotranspiration), soil salinity and sodicity variables (EC, and ESP), terrain (elevation and slope), hydrology (drainage and canal system), and bio-physical variables (LST and LULC). Salinity and aridity are globally recognized as significant contributors to land degradation and deterioration of soil quality across various regions worldwide. These factors pose significant challenges to agricultural productivity, natural ecosystems, and overall land sustainability (Pravalie et al., 2021). Their adverse effects on soil health and fertility have been observed in diverse climatic zones, ranging from regional to global regions and beyond. Understanding the impacts of salinity and aridity on land and soil is significant for implementing effective measures to combat land degradation and promote soil sustainable management practices on a global and micro region (Perri et al., 2022; Thiam et al., 2021).

Figure 1 VOS Viewer map of the author's keywords addressing land degradation issues

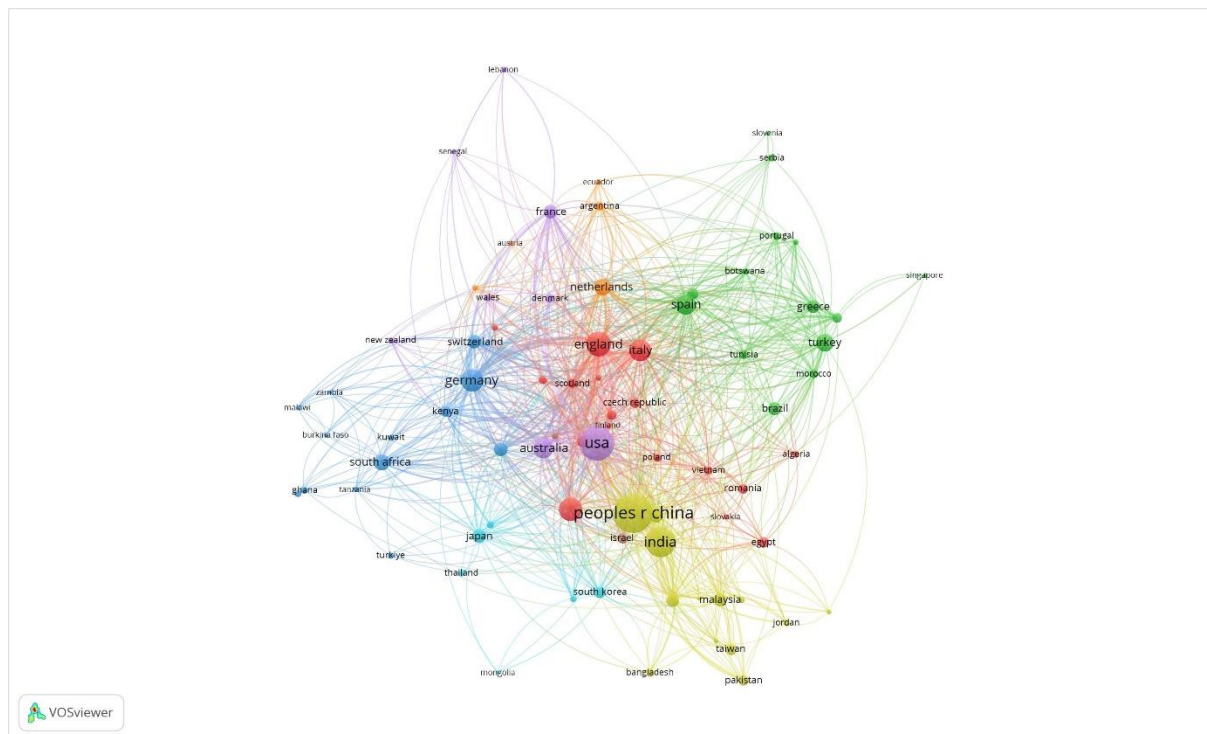


Figure 2 Map depicting collaborative efforts among countries in addressing land degradation issues

Extensive research efforts have been dedicated to studying different types of land degradation, including water erosion, gully erosion, and wind erosion. However, there has been a notable gap in research when it comes to identifying and addressing the specific challenges of salinity and aridity (rainfall and evapotranspiration) degradation in arid and semi-arid regions. To better understand and combat land degradation at micro level, there is a need for more comprehensive and integrated approaches that utilize geospatial data and advanced modeling techniques provided by tools like MCDA in the GIS environment. The utilization of geospatial techniques, including remote sensing (RS) datasets and geographical information system (GIS), has become increasingly prevalent and valuable in the modeling and evaluation of land degradation process. These advanced technologies offer robust capabilities for acquiring, analysing, and visualizing geospatial data, enabling researchers and land expert to gain a deeper understanding of the dynamics of land degradation processes. The integration of RS and GIS provides a comprehensive and efficient approach for studying the intricate interactions among various factors contributing to land degradation. This integration facilitates informed decision-making and the formulation of effective land management strategies (Abuzaid et al., 2021).

In this study, our primary focus was on the assessment of land degradation caused by salinity/sodicity and aridity condition, specifically examining its consequences on soil salinity and aridity. The aims of the study were (1) to analyse and understand the biophysical, climate, terrain, and soil characteristics of the study area, in order to gain a comprehensive understanding of its environmental conditions and (2) to identify the susceptible agriculture fields affected by salinity/aridity at the Mashi dam command area, India using combination of AHP and geospatial datasets.

2. Materials and Methods

2.1. Study Area

Mashi command area, is the minor irrigation project in Rajasthan, India, spans a geographical area between latitude $26^{\circ} 16' N$ to $26^{\circ} 41' N$ and longitude $75^{\circ} 65' E$ to $75^{\circ} 76' E$, as depicted in Figure 3. The command area is located under the Chambal River Basin in the south, with the majority situated in the Banas River Basin, and covers an extensive area of 90.07 km^2 . A major part of the Mashi dam catchment lies under Jaipur, Ajmer, and Tonk district. It has three tributaries: Bandi, Mashi, and Sohadara, all rivers drop down in Banas River Basin. The

area is characterized by its semi-arid climate, with limited rainfall and high evapotranspiration rates. The region showcases a variety of soil types, including alluvial soils, sandy soils, and clayey soils, each with their specific characteristics and suitability for different crops. The soil fertility, moisture retention capacity, and nutrient content significantly influence the agricultural practices and cropping patterns in the area. The Mashi Dam command area has peneplain topography, with a ground elevation ranging from 160 to 300 meters above mean sea level. Hillocks can be found in isolation as well as in continuous chains in the southeast near Galod. Undulated topography is found near the left bank of the Mashi River (Ground water Atlas, Tonk District).

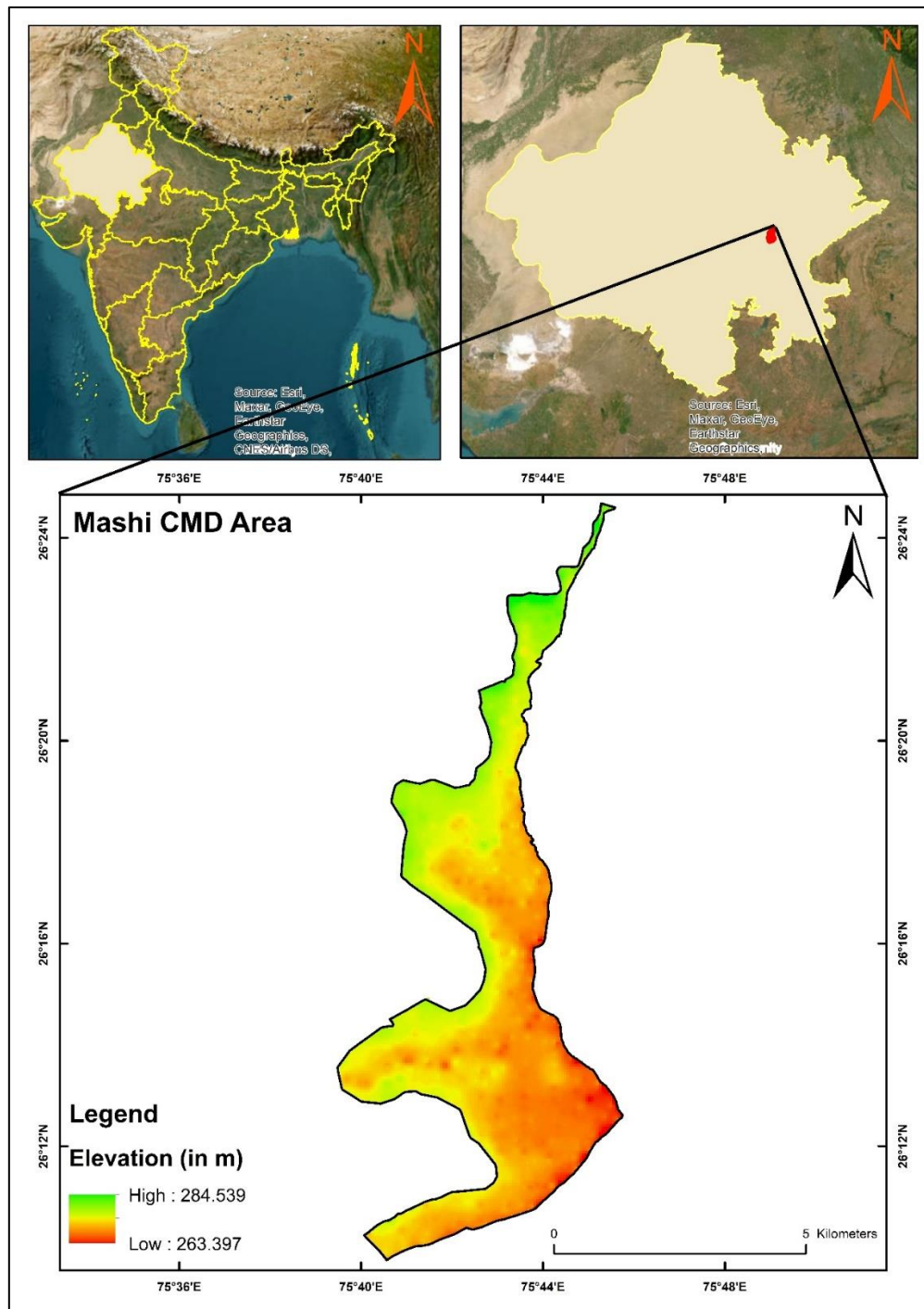


Figure 3 Study site map of Mashi Dam Command Area, Rajasthan, India

2.2. Data Collection and Processing

In order to gather the necessary data for this study, we were utilized ten sensitive data layers to identify the vulnerable area from land degradation. For this purpose, we were accessed the Copernicus open access hub website to download Sentinel 2A MSI image for the time period 2018 and this image was utilized to prepare land use/land cover (LULC) map of the study area (<https://dataspace.copernicus.eu>). Additionally, we obtained Cartosat DEM (2.5 m) from the Bhuvan, NRSC platform to collect information about the elevation and slope of the study area (<https://bhuvan-app3.nrsc.gov.in>). For the time periods from 1988 to 2018, we were acquired bio-physical variable such as mean annual land surface temperature (LST) as well as climate parameters (mean annual precipitation, and mean annual evapotranspiration) using Climate engine platform. The Climate Engine platform facilitated the extraction of this data with the help of Google Earth engine (<https://app.climateengine.org/climateEngine>). To assessment of land degradation vulnerability in the study area, we analysed the specific data (precipitation, land surface temperature and evapotranspiration) over a 30-year period, providing a comprehensive view of long-term trends. To complement our analysis, we conducted laboratory experiments to obtain physical and chemical properties of soil from soil samples. These measurements played a significant role in understanding the soil characteristics within the study area. To ensure consistency across the data layers, we converted all thematic layers to the WGS 1984 datum and utilized the Universal Transverse Mercator (UTM) 43N coordinate system as well as for similar pattern of all datasets were convert 30 m resolution. For a detailed overview of the datasets employed in our study, are provided in Table 1, which includes specifications and descriptions of the various datasets used. The comprehensive methodological framework and analysis for the entire study are depicted in Figure 4.

Table 1 Datasets used in the study

| Sl. No. | Variables /factors | Datasets | Sources/methods |
|---------|----------------------|----------------------------|---|
| 1 | Soil EC | Soil samples (2018) | measurement in laboratory by EC meter |
| 2 | Soil ESP | Soil samples (2018) | measurement in laboratory by chemical method |
| 3 | Elevation | Cartosat-1 DEM | (https://bhuvan-app3.nrsc.gov.in) |
| 4 | Slope | Cartosat-1 DEM | (https://bhuvan-app3.nrsc.gov.in) |
| 5 | Mean annual rainfall | Terra climate (1988-2018) | (https://app.climateengine.org/climateEngine) |
| 6 | Mean annual PET | Terra climate (1988-2018) | (https://app.climateengine.org/climateEngine) |
| 7 | Mean annual LST | Landsat series (1988-2018) | (https://app.climateengine.org/climateEngine) |
| 8 | LULC | Sentinel 2A (2018) | (https://dataspace.copernicus.eu) |
| 9 | Drainage | - | Ground water Atlas, Tonk District |
| 10 | Canal system | - | District irrigation report, Tonk |

EC: Electrical conductivity, ESP: Exchangeable sodium percentage, PET: Potential Evapotranspiration, LST: Land surface temperature, LULC: Land-use/land-cover.

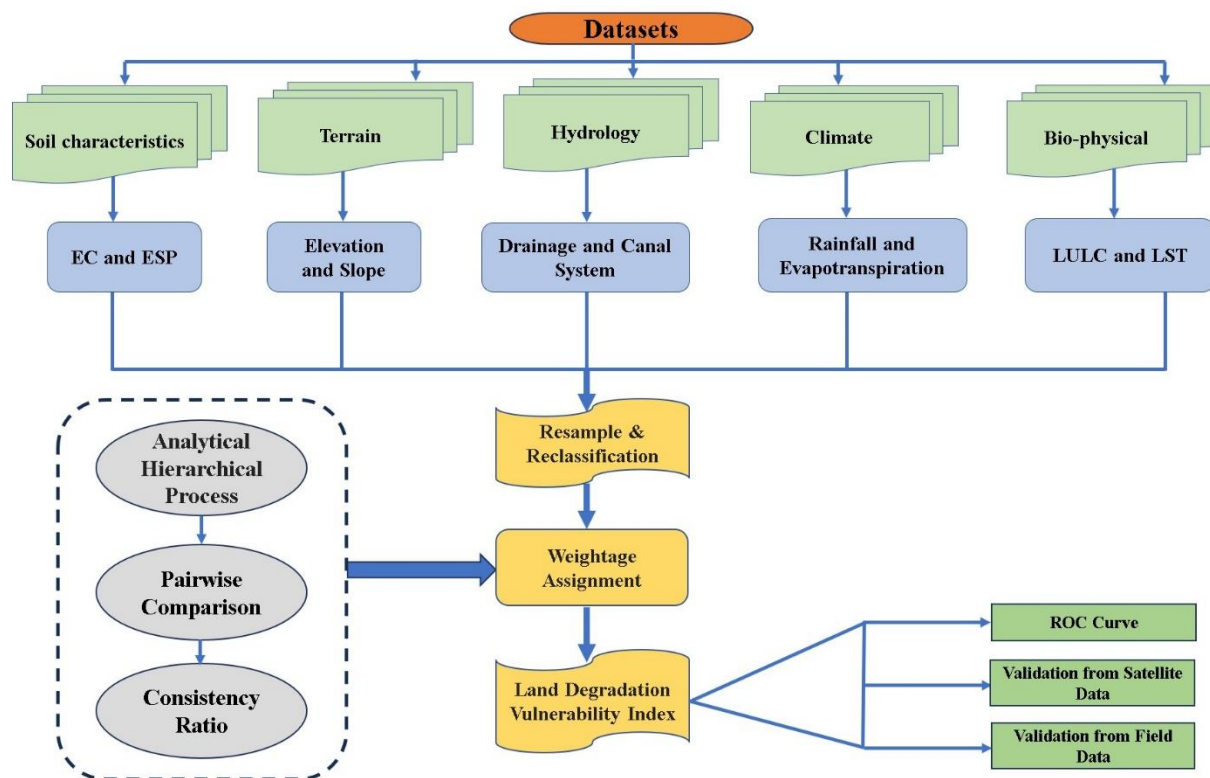


Figure 4 Flowchart of the methodology followed in the study

2.3. Analytical hierarchical process (AHP) and weightage assessment

The Analytical Hierarchical Process (AHP) technique, employed within the framework of multi-criteria decision analysis (MCDA), is widely recognized as a prominent method for evaluating land degradation vulnerability (Mzuri et al., 2022). AHP is based on a pairwise comparison assessment theory, utilizing Saaty's scale of relative importance to compare different parameters (Table 2). By making these comparisons and assigning numerical values that signify the importance of one parameter relative to another within a specific criterion, we can systematically draw informed conclusions regarding priorities. This enables us to establish a structured approach in evaluating land degradation vulnerability and effectively prioritize the factors contributing to it.

Table 2 Saaty's, 1980 scale (1–9) for pairwise comparison in AHP

| Scale | Scale importance |
|-------|------------------------------------|
| 1 | Equal importance |
| 2 | Intermediate between scale 1 and 3 |
| 3 | Moderate importance |
| 4 | Intermediate between scale 3 and 5 |
| 5 | Strong importance |
| 6 | Intermediate between scale 5 and 7 |
| 7 | Very strong importance |
| 8 | Intermediate between scale 7 and 9 |

The validation of pairwise comparisons for the different thematic layers and their subclasses was conducted using the consistency ratio (CR). By employing the CR, we were able to assess the consistency of the pairwise comparisons and ensure the reliability of the decision-making process. This validation step helps to enhance the accuracy and robustness of the analysis by evaluating the coherence and agreement among the compared parameters. The CR was calculated using the following formula (Eq. 1):

$$CR = \frac{CI}{RI} \quad (1)$$

Where RI indicates the random consistency index, and Saaty's (1980) standard is used to calculate its values (Table 3); CI stands for the consistency index, which was calculated using the following formula (Eq. 2):

$$CI = \frac{(\lambda_{\max} - n)}{(n-1)} \quad (2)$$

Where λ_{\max} indicates the principal eigenvalue, and n indicates the total number of input criteria used in the LD assessment.

Table 3 Saaty's random consistency index

| N | 1 | 2 | 3 | 4 | 5 | 6 | 7 | 8 | 9 | 10 | 11 | 12 | 13 | 14 |
|-----|---|---|------|-----|------|------|------|------|------|------|------|------|------|------|
| RCI | 0 | 0 | 0.58 | 0.9 | 1.12 | 1.24 | 1.32 | 1.41 | 1.45 | 1.49 | 1.51 | 1.48 | 1.56 | 1.57 |

N-order of the matrix, RCI-random consistency index.

ArcGIS utilized Inverse Distance Weighted (IDW) interpolation and Euclidean distance methods to generate surface maps of soil EC, ESP, drainage, and canal systems. In the spatial analysis tool of ArcGIS, the key determinant factors or themes influencing land degradation underwent reclassification. This involved assigning values (ranging from 1 to 9), or criteria, using the scale proposed by Saaty (1980). This process facilitated the transformation of original values into weighted values based on their respective degrees of influence on land degradation, as outlined in Table 3.

During the weighted overlay analysis using the analytical hierarchical process (AHP), an acceptable threshold for the consistency ratio (CR) is set at ≤ 0.10 . If the CR exceeds this threshold, it indicates an inconsistency in the decision-making process. In such cases, it becomes necessary to revisit the decision and identify the source of the inconsistency. By addressing and resolving the underlying issues, the goal is to ensure that the CR value falls below 0.10. This rigorous approach helps to maintain the integrity and reliability of the weighted overlay analysis, ensuring that the final decision reflects a consistent and robust assessment of the data.

2.4. Land Degradation Vulnerability Index (LDVI)

To delineate the land degradation vulnerability (LDV) areas at the command area, all thematic layers and their sub-categories were assigned weightages based on the Analytical Hierarchical Process (AHP) and, spatial analysis tool (ArcGIS software) was used to prepare geo-spatial map of LDV at the study area. The LDV map was generated using below equation specified in the study (Eq. 3).

$$LDVI = EC * 0.22 + ESP * 0.15 + LULC * 0.13 + Slope * 0.12 + Elevation * 0.08 + ETo * 0.08 + Rainfall * 0.07 + LST * 0.05 + Drainage * 0.05 + Canal * 0.03 \quad (3)$$

Subsequently, the LDV index was categorized into three classes, namely, slightly vulnerable, moderately vulnerable, and highly vulnerable utilizing reclassify tool in ArcGIS. To validate the LDV map, six randomly selected sites were examined using high resolution Google Earth imagery. Additionally, a receiver operating characteristic (ROC) curve was created based on fifty randomly selected points using Google Earth, allowing the estimation of the area under the curve (AUC). AUC values range between 0.5 and 1, where values closer to 1 indicate excellent model performance, while values closer to 0.5 indicate poor prediction accuracy. Furthermore,

field's shots were used to validate the LDV map generated through the AHP and weightage method, assessing the level of agreement between the field observations and the predicted map from the model. Through these validation processes, the study aimed to assess the accuracy and reliability of the LDV map, ensuring its effectiveness in representing the actual land degradation vulnerability within the study area.

3. Results and Discussions

In this analysis, we incorporated ten variables inclusive of electrical conductivity (EC), exchangeable sodium percentage (ESP), Elevation, Slope, Drainage, Canal system, Rainfall, Potential Evapotranspiration (PET), LULC, and land surface temperature (LST). The study was focused on the minor irrigation project of Mashi dam command area, Rajasthan, India.

In this analysis, we incorporated ten variables inclusive of electrical conductivity (EC), exchangeable sodium percentage (ESP), Elevation, Slope, Drainage, Canal system, Rainfall, Potential Evapotranspiration (PET), LULC, and land surface temperature (LST). The study was focused on the minor irrigation project of Mashi dam command area, Rajasthan, India.

3.1. Soil characteristics (EC and ESP)

Electrical conductivity and the exchangeable sodium percentage (ESP) plays a significant role in the land degradation process as it serves as an indicator of soil salinity and sodicity. High EC and ESP often indicates an elevated concentration of dissolved salts, and the proportion of sodium ions on the exchange sites of soil particles, which can adversely impact particularly in relation to soil structure, fertility and overall health (Pessoa et al., 2022). In this research work, Electrical Conductivity (EC) and Exchangeable Sodium Percentage (ESP) concentrations were obtained by measuring soil samples in the environmental laboratory. Subsequently, EC and ESP sub-categories were generated based on the obtained data using the natural break method and reclassify tool in ArcGIS. The observed EC ranged from 7.99 to 15.46 dS/m, while ESP ranged from 9.80% to 11.43%. Both variables were classified into five classes: Very low (7.99–9.81 dS/m), low (9.81–11.04 dS/m), moderate (11.04–12.24 dS/m), high (12.24–13.62 dS/m), and very high (13.62–15.46 dS/m). Similarly, ESP was categorized into five classes: Very low (9.80–10.38%), low (10.38–10.62%), moderate (10.62–10.82%), high (10.82–11.06%), and very high (11.06–11.43%). The corresponding maps for EC and ESP are presented in Figure 5 (A and B). The AHP method was employed to calculate the weightage and consistency ratio for main criteria and sub-criteria of EC and ESP layers. In this study, sub-criteria characterized by low Electrical Conductivity (EC) and Exchangeable Sodium Percentage (ESP) values were assigned lower weights, while conversely, subcategories exhibiting high EC and ESP values were assigned high weights (Table 4).

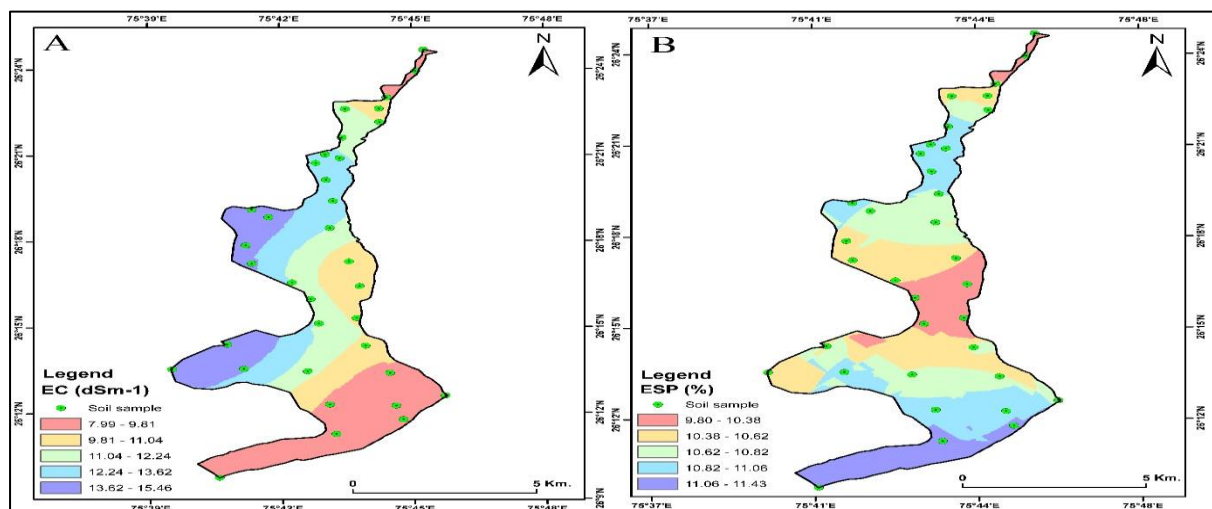


Figure 5 Land degradation criteria for Mashi CMD Area (A. EC, B. ESP)

3.2. Terrain characteristics (Elevation and slope)

Elevation and slope are topographical factors that significantly influence the land degradation process. Their roles are interconnected and can impact various aspects of soil and landscape dynamics. Elevation and slope gradient influence the speed of water runoff during precipitation events. High slopes can lead to rapid runoff, increasing the risk of flooding, which may result in soil erosion, sedimentation, and the degradation of downstream areas. The removal of natural vegetation, through factors like sand mining, deforestation or improper land use, on high slopes can increase the risk of soil erosion and land degradation (Jaafari et al., 2022). In this work, the Cartosat-1 DEM data (10 m) was utilized to generate elevation and slope thematic map. The elevation range in the study area spanned from 263.39 to 284.53 m, categorized into five classes: very low (263.39-270.44 m), low (270.44-272.76 m), moderate (272.76-275.33 m), high (275.33-278.32 m), and very high (278.32-284.53 m). For slope layer construction, the Cartosat-1 DEM data was employed to generate slope percentages, which were subsequently categorized into five classes: very low (0–0.14%), low (0.14–0.28%), moderate (0.28–0.45%), high (0.45–0.70%), and very high (0.70–1.40%). The corresponding elevation and slope maps are depicted in Figure 6 (C and D). The AHP method was employed to calculate the weightage and consistency ratio for main criteria and sub-criteria of elevation and slope layers. In this study, sub-criteria characterized by low elevation and slope were assigned low weights, while conversely, subcategories exhibiting high elevation and slope values were assigned higher weights (Table 4).

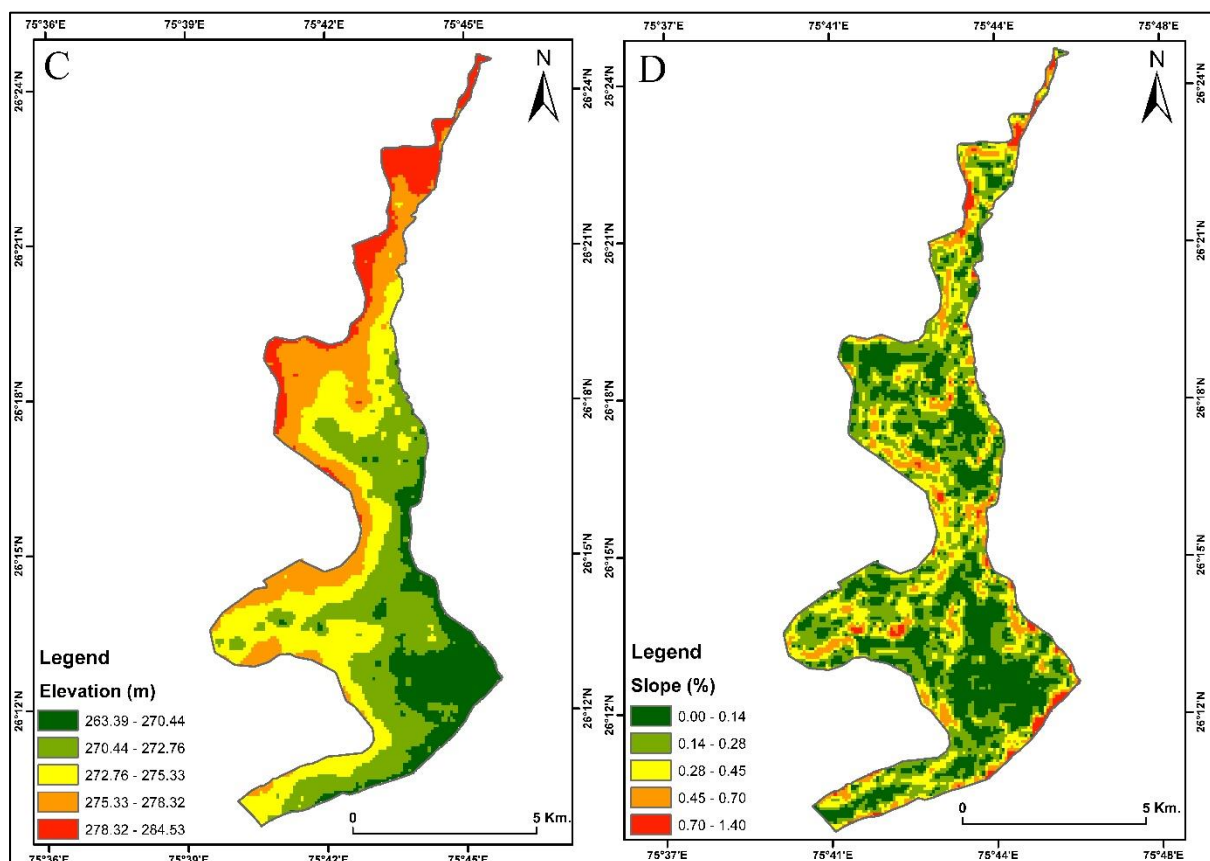


Figure 6 Land degradation criteria for Mashi CMD Area (C. Elevation, D. Slope)

3.3. Hydrology characteristics (Drainage and Canal systems)

The role of drainage and canal systems in the land degradation process is complex and depends on factors such as design, maintenance, and regional characteristics. While properly designed and managed drainage and canal systems can contribute to sustainable land use, improper planning and management of canal system can result in waterlogging, especially in poorly drained soils. Waterlogged conditions contribute to soil compaction, reduced

aeration, and decreased soil fertility, leading to land degradation (Mohamed et al., 2019). For this analysis, we were prepared drainage and canal network from the secondary datasets (ground water atlas and District irrigation report, Tonk). After that for surface generation, we were used Euclidean distance tool in ArcGIS. The study area drainage and canal system were classified into five sub-classes: Very Poor, Poor, Moderate, High, and Excessive. The corresponding drainage and canal maps are depicted in Figure 7 (E and F). The AHP method was employed to calculate the weightage and consistency ratio for main criteria and sub-criteria of drainage and canal layers. In this study, sub-criteria characterized by Very Poor drainage and canals values were assigned lower weights, while conversely, subcategories exhibiting Excessive drainage and canals values were assigned higher weights (Table 4).

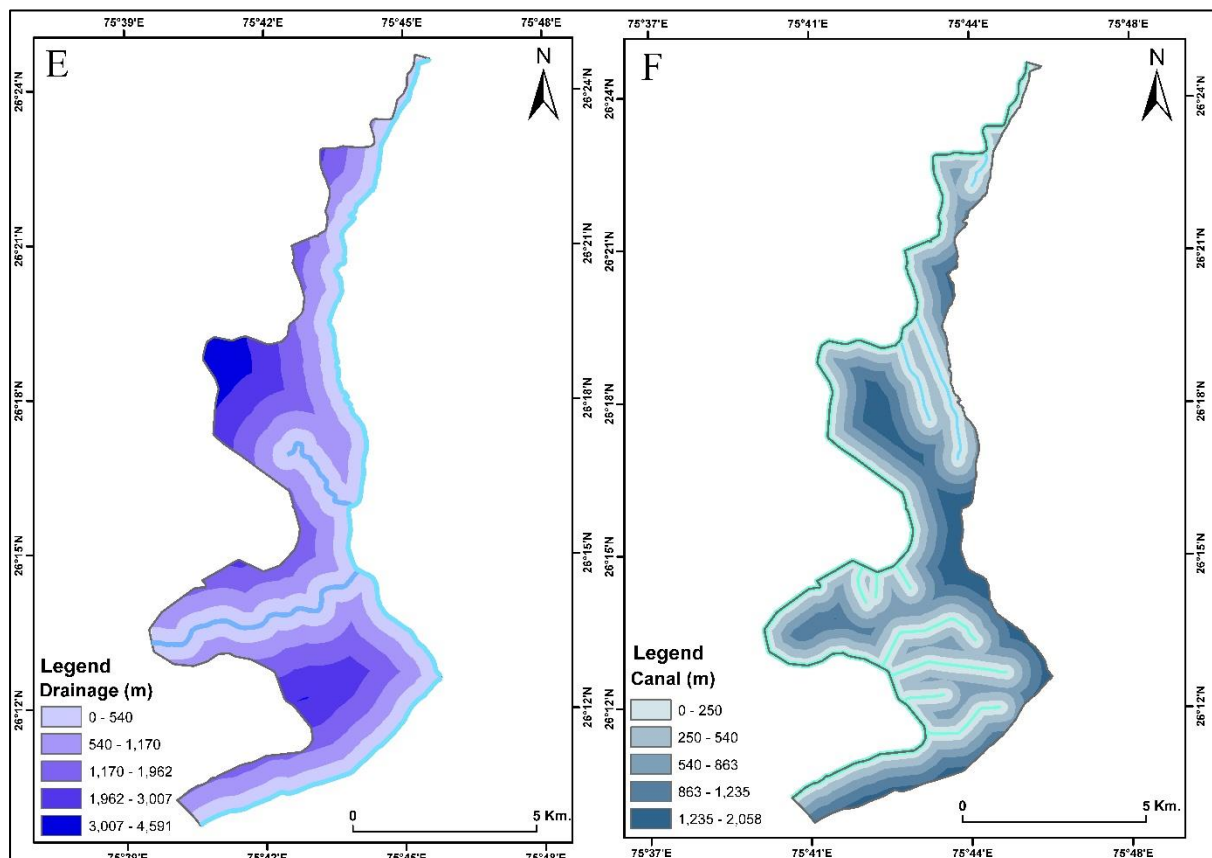


Figure 7 Land degradation criteria for Mashi CMD Area (E. Drainage, F. Canal systems)

3.4. Climate characteristics (Rainfall and Evapotranspiration)

Rainfall plays an important role in the land degradation process, influencing soil erosion, vegetation health, and overall ecosystem stability. In arid and semi-arid regions, insufficient rainfall contributes to drought, soil dryness, reduced vegetation cover, and increased vulnerability to wind and water erosion. Due to drought conditions resulting to reduced plant growth, while high rainfall may cause flooding and negatively impact vegetation and soil health (Shao et al., 2024). The average annual rainfall was classified into five subclasses: very low (200–250 mm), low (250–300 mm), moderate (300–350 mm), high (350–600 mm), and very high (600–900 mm), covering approximately 3%, 5%, 20%, 42%, and 30% of the total geographical area, respectively. The eastern lower command area of the study area receives very high precipitation, while the western main canal part experiences very low rainfall. Potential evapotranspiration (PET) is an important factor of the water cycle that includes both evaporation from the soil surface and transpiration from plant surfaces. While PET itself does not directly cause land degradation, it plays a significant role in influencing soil moisture dynamics, vegetation health, and overall ecosystem resilience (Goroshi et al., 2017). The average annual PET was classified into five subclasses: very low (50–100 mm), low (100–200 mm), moderate (200–300 mm), high (300–400 mm), and very high (400–600 mm),

covering approximately 3%, 5%, 30%, 20%, and 42% of the total geographical area, respectively. Aridity, high EC, and ESP collectively contribute to stress on vegetation and soil properties. Water scarcity, salinity, and sodicity conditions can lead to reduced plant growth, increased vulnerability to pests and diseases, and diminished vegetation cover, further contributing to land degradation. The corresponding rainfall and evapotranspiration maps are depicted in Figure 8 (G and H). The AHP method was employed to calculate the weightage and consistency ratio for main criteria and sub-criteria of rainfall and evapotranspiration layers. In this study, sub-criteria characterized by low rainfall and evapotranspiration values were assigned higher weights, while conversely, subcategories exhibiting high rainfall and evapotranspiration values were assigned lower weights (Table 4).

Table 4 Scaling of criteria based on AHP pairwise comparison

| Main Criteria | EC | ESP | LULC | Slope | Elevation | PET | Rainfall | LST | Drainage | Canal |
|---------------|------|------|------|-------|-----------|-------|----------|-------|----------|-------|
| EC | 1 | 3 | 2 | 3 | 3 | 3 | 3 | 5 | 2 | 5 |
| ESP | 0.33 | 1 | 3 | 2 | 2 | 3 | 2 | 3 | 2 | 3 |
| LULC | 0.50 | 0.33 | 1 | 2 | 3 | 3 | 3 | 2 | 2 | 3 |
| Slope | 0.33 | 0.50 | 0.50 | 1 | 3 | 3 | 2 | 3 | 2 | 3 |
| Elevation | 0.33 | 0.50 | 0.33 | 0.33 | 1 | 2 | 3 | 2 | 2 | 2 |
| PET | 0.33 | 0.33 | 0.33 | 0.33 | 0.50 | 1 | 3 | 3 | 2 | 2 |
| Rainfall | 0.33 | 0.50 | 0.33 | 0.50 | 0.33 | 0.33 | 1 | 2 | 3 | 3 |
| LST | 0.20 | 0.33 | 0.50 | 0.33 | 0.50 | 0.33 | 0.50 | 1 | 2 | 3 |
| Drainage | 0.50 | 0.50 | 0.50 | 0.50 | 0.50 | 0.50 | 0.33 | 0.50 | 1 | 2 |
| Canal | 0.20 | 0.33 | 0.33 | 0.33 | 0.50 | 0.50 | 0.33 | 0.33 | 0.50 | 1 |
| Sum | 4.07 | 7.33 | 8.83 | 10.33 | 14.33 | 16.67 | 18.17 | 21.83 | 18.50 | 27.00 |

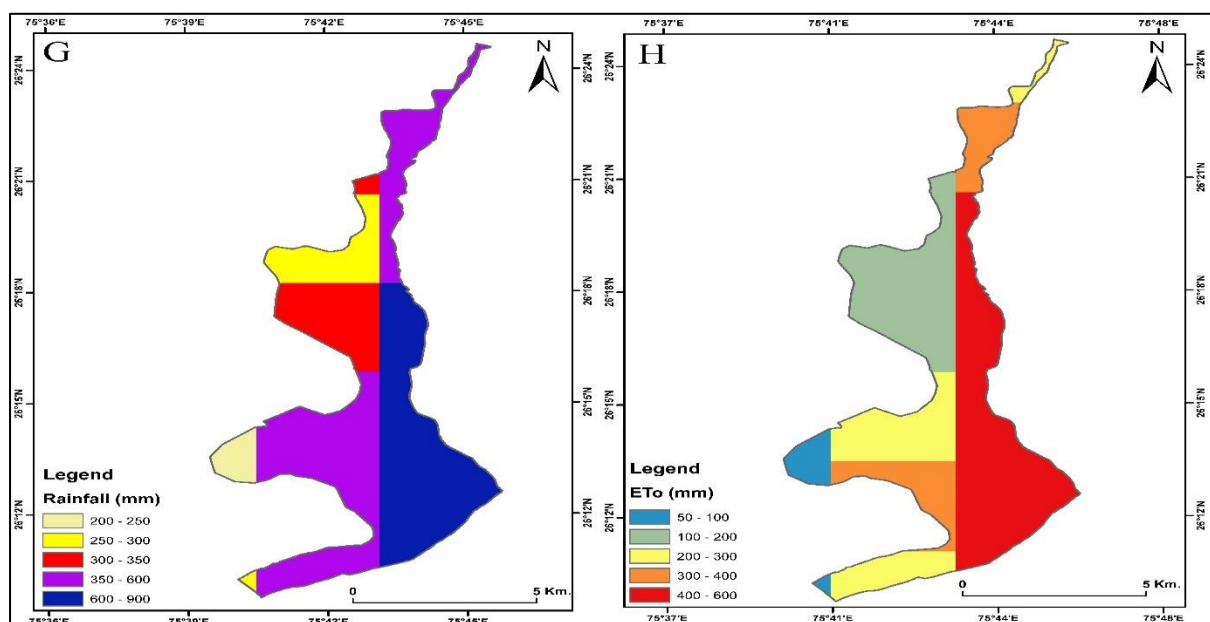


Figure 8 Land degradation criteria for Mashi CMD Area (G. Rainfall, H. Evapotranspiration)

3.5. Bio-physical characteristics (LULC and LST)

Land-use and land-cover (LULC) dynamics are predominantly accelerated by anthropogenic and human activities, resulting in various changes that impact land and the ecosystem. Several research scholars have emphasized the significance of LULC in assessing the land degradation process (Ahmad and Pandey, 2018; Mashame and Akinyemi, 2016). The predominant cause of land degradation in irrigated areas is attributed to excessive irrigation practices and waterlogging. As per the change analysis of LULC from 1988 to 2018, mostly irrigated lands are changing to barren land due to the human induced practices (over-irrigation) in irrigated lands. This ongoing process is contributing to alterations in soil quality and fertility. In this work, LULC has been classified into six distinct classes: barren land, built-up land, crop land, sandy area, scrub land, and water bodies. Crop land follows with 72.29 sq. km. (80.26%), sandy areas with 1.79 sq. km. (1.99%), scrub lands with 2.33 sq. km. (2.58%), barren land areas with 8.26 sq. km. (9.17%), settlement areas with 4.83 sq. km. (5.37%), and water bodies comprising 0.56 sq. km. (0.62%) across the study region.

Significance and understanding the role of land surface temperature in land degradation process is essential for developing planning to diminish its impact. Monitoring temperature patterns, especially in conjunction with other environmental variables, (LULC, PET, EC and ESP) can provide valuable info into the dynamics of land degradation and sustainable land management practices (Roy et al., 2023). For this analysis, we were extracted annual averaged LST data from 1988 to 2018 using climate engine web-portal. The study area land surface temperature was categorized into five sub-classes: 30–35, 35–37, 37–38, 38–39, and 39–42°C. The first and second subclass (from 30–35 °C to 35–37 °C), representing lower temperatures, covers mainly in the eastern lower part of the CMD area. The third subclass (37–38°C) is predominantly distributed in the northern and eastern parts of the CMD area. Approximately 75% of the CMD area is covered by the fourth and fifth subclasses of land surface temperature (38–39, 39–42 °C), predominantly situated in the western and central regions of the study area. The AHP method was employed to calculate the weightage and consistency ratio for main criteria and sub-criteria of LULC and LST layers. In this analysis, sub-criteria characterized by low LST values were assigned low weights, while conversely, subcategories exhibiting high LST values were assigned higher weights. The corresponding LULC and LST maps are depicted in Figure 9 (I and J).

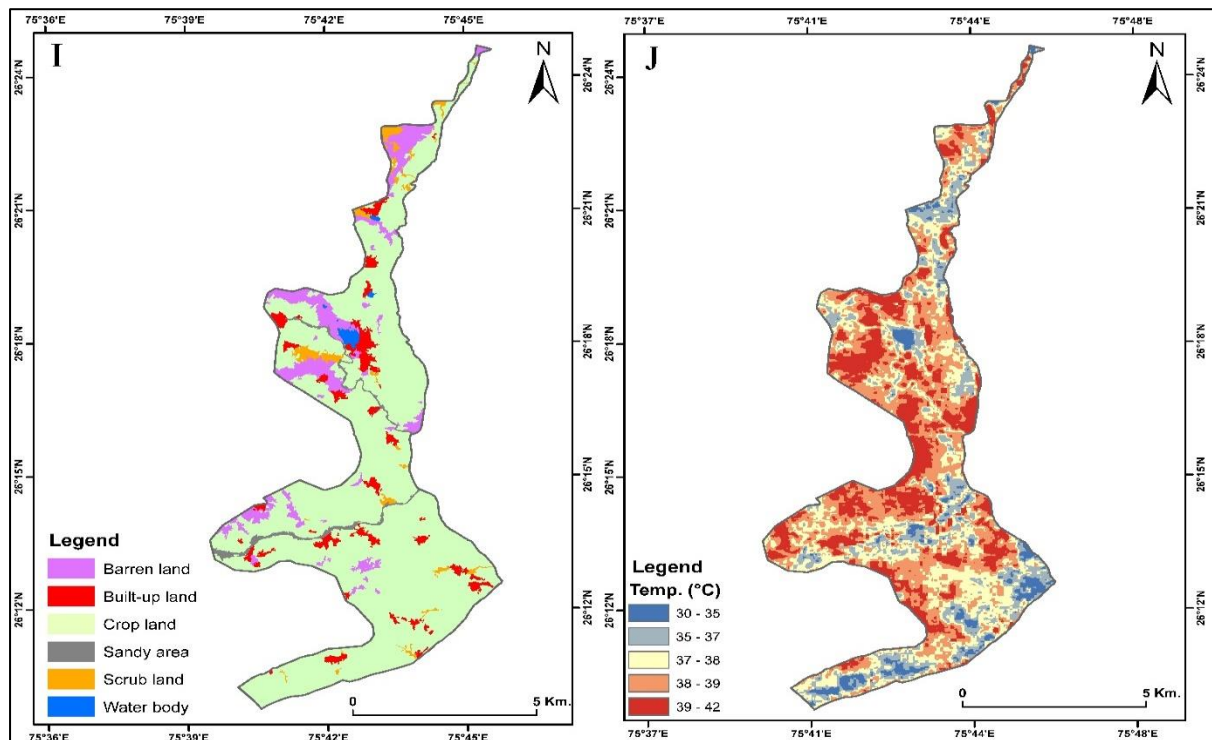


Figure 9 Land degradation criteria for Mashi CMD Area (I. LULC, J. LST)

3.6. Analytical Hierarchy Process (AHP) Analysis

Table 5 and 6 shows the pair-wise comparison matrix for the ten determinant factors (main criteria) influencing land degradation vulnerability in CMD area. Among the factors considered for land degradation, EC and ESP has much larger eigen weight (0.22, and 0.15) than other eight criteria. The absolute weights of other factors like LULC, slope, elevation, and PET are about 0.13, 0.12, 0.08 and 0.08, respectively. On the contrary, the rainfall (0.07), LST (0.05), drainage (0.05) and canal system (0.03) had very low weights. The Consistency ratio (CR) value in this study was found to be 0.08, which is less than 0.10, thus results confirmed the weights attributed were suitable and reliable (Table 7).

Table 5 Normalized pairwise Matrix and criteria weight estimation

| Main Criteria | EC | ESP | LULC | Slope | Elevation | PET | Rainfall | LST | Drainage | Canal | Criteria Weight |
|---------------|----------|----------|----------|----------|-----------|----------|----------|----------|----------|----------|-----------------|
| EC | 0.25 | 0.41 | 0.23 | 0.29 | 0.21 | 0.18 | 0.17 | 0.23 | 0.11 | 0.19 | 0.22 |
| ESP | 0.08 | 0.14 | 0.34 | 0.19 | 0.14 | 0.18 | 0.11 | 0.14 | 0.11 | 0.11 | 0.15 |
| LULC | 0.12 | 0.05 | 0.11 | 0.19 | 0.21 | 0.18 | 0.17 | 0.09 | 0.11 | 0.11 | 0.13 |
| Slope | 0.08 | 0.07 | 0.06 | 0.10 | 0.21 | 0.18 | 0.11 | 0.14 | 0.11 | 0.11 | 0.12 |
| Elevation | 0.08 | 0.07 | 0.04 | 0.03 | 0.07 | 0.12 | 0.17 | 0.09 | 0.11 | 0.07 | 0.08 |
| PET | 0.08 | 0.05 | 0.04 | 0.03 | 0.03 | 0.06 | 0.17 | 0.14 | 0.11 | 0.07 | 0.08 |
| Rainfall | 0.08 | 0.07 | 0.04 | 0.05 | 0.02 | 0.02 | 0.06 | 0.09 | 0.16 | 0.11 | 0.07 |
| LST | 0.05 | 0.05 | 0.06 | 0.03 | 0.03 | 0.02 | 0.03 | 0.05 | 0.11 | 0.11 | 0.05 |
| Drainage | 0.12 | 0.07 | 0.06 | 0.05 | 0.03 | 0.03 | 0.02 | 0.02 | 0.05 | 0.07 | 0.05 |
| Canal | 0.05 | 0.05 | 0.04 | 0.03 | 0.03 | 0.03 | 0.02 | 0.02 | 0.03 | 0.04 | 0.03 |
| Total | 1 | 1 | 1 | 1 | 1 | 1 | 1 | 1 | 1 | 1 | 1 |

Table 6 Calculating and check Consistency ratio of parameters

| Main Criteria | EC | ESP | LULC | Slope | Elevation | PET | Rainfall | LST | Drainage | Canal | λ_{max} | Consistency Index | Random Index | Consistency Ratio |
|---------------|------|------|------|-------|-----------|------|----------|------|----------|-------|-----------------|-------------------|--------------|-------------------|
| EC | 0.22 | 0.46 | 0.27 | 0.35 | 0.25 | 0.23 | 0.21 | 0.27 | 0.11 | 0.16 | | | | |

| | | | | | | | | | | | | | | |
|-------|----|----|-----|-----|------|----|------|----|------|-----|-----|------|------|------|
| | 0. | 0. | 0.4 | 0.2 | | 0. | | 0. | | 0.1 | | | | |
| ESP | 07 | 15 | 0 | 3 | 0.17 | 23 | 0.14 | 16 | 0.11 | 0 | | | | |
| LUL | 0. | 0. | 0.1 | 0.2 | | 0. | | 0. | | 0.1 | | | | |
| C | 11 | 05 | 3 | 3 | 0.25 | 23 | 0.21 | 11 | 0.11 | 0 | | | | |
| | 0. | 0. | 0.0 | 0.1 | | 0. | | 0. | | 0.1 | | | | |
| Slope | 07 | 08 | 7 | 2 | 0.25 | 23 | 0.14 | 16 | 0.11 | 0 | | | | |
| Eleva | 0. | 0. | 0.0 | 0.0 | | 0. | | 0. | | 0.0 | 11. | 0.12 | 1.49 | 0.08 |
| tion | 07 | 08 | 4 | 4 | 0.08 | 16 | 0.21 | 11 | 0.11 | 7 | 11 | | | |
| | 0. | 0. | 0.0 | 0.0 | | 0. | | 0. | | 0.0 | | | | |
| PET | 07 | 05 | 4 | 4 | 0.04 | 08 | 0.21 | 16 | 0.11 | 7 | | | | |
| Rainf | 0. | 0. | 0.0 | 0.0 | | 0. | | 0. | | 0.1 | | | | |
| all | 07 | 08 | 4 | 6 | 0.03 | 03 | 0.07 | 11 | 0.16 | 0 | | | | |
| | 0. | 0. | 0.0 | 0.0 | | 0. | | 0. | | 0.1 | | | | |
| LST | 04 | 05 | 7 | 4 | 0.04 | 03 | 0.03 | 05 | 0.11 | 0 | | | | |
| Drain | 0. | 0. | 0.0 | 0.0 | | 0. | | 0. | | 0.0 | | | | |
| age | 11 | 08 | 7 | 6 | 0.04 | 04 | 0.02 | 03 | 0.05 | 7 | | | | |
| Canal | 0. | 0. | 0.0 | 0.0 | | 0. | | 0. | | 0.0 | | | | |
| 1 | 04 | 05 | 4 | 4 | 0.04 | 04 | 0.02 | 02 | 0.03 | 3 | | | | |

Table 7 Land degradation vulnerability classes and area

| Sl. No. | LDVI Classes | Area (in km ²) | Area (in %) |
|---------|-----------------------|----------------------------|-------------|
| 1 | Slightly vulnerable | 36.26 | 40.26 |
| 2 | Moderately vulnerable | 46.94 | 52.12 |
| 3 | Highly vulnerable | 6.87 | 7.63 |

3.7. Land degradation vulnerability index (LDVI)

The Land Degradation Vulnerability Index (LDVI) for the Mashi Dam Command (CMD) area was established by integrating geo-spatial layers of soil sample derived electrical conductivity (EC) and exchangeable sodium percentage (ESP), Terra climate derived precipitation and evapotranspiration data, elevation and slope derived from Cartosat-1 DEM, and Land Use/Land Cover (LULC) information obtained from Sentinel 2A image, along with secondary datasets like drainage and canal systems. Geospatial techniques, specifically applying the analytic hierarchy process (AHP), were employed in the development of LDVI. According to the analytic hierarchy process (AHP), the predominant factors influencing land degradation vulnerability (LDV) in the investigated area were the chemical and physical properties of the soil (EC and ESP), collectively accounting for 0.37 of the total weights. The Land Degradation Vulnerability Index (LDVI) was classified into three classes: highly vulnerable, moderately vulnerable, and slightly vulnerability areas. The AHP and GIS-based results (Table 8) indicated that 52.12% (46.94 km²) of the study area is moderately vulnerable to land degradation, primarily in the western, and upper part of the CMD area. About 7.63% (6.87 km²) of the area is highly vulnerable, particularly in the western and central part of the main canal, while 40.26% (36.26 km²) is classified as very slightly vulnerable, mainly in the northern and western southern parts of the study area. LDVI classified area statistics is also shown in Figure 10. These findings provide valuable information for local decision makers to targeted soil conservation and management at the large and micro scale land hazard concerns in future planning initiatives.

Table 8 Weights and consistency ration of the sub-criteria for assessment of land degradation vulnerability index

| Main Criteria | Weight | Consistency Ratio | Sub-Criteria | Sub-criteria Rank | Weight | Consistency Ratio |
|---------------|--------|-------------------|--------------|-------------------|--------|-------------------|
| EC (dS/m) | 0.22 | 0.08 | Very low | 1 | 0.06 | 0.07 |
| | | | low | 2 | 0.12 | |
| | | | Moderate | 3 | 0.20 | |
| | | | High | 4 | 0.26 | |
| | | | Very high | 5 | 0.35 | |
| ESP (%) | 0.15 | | Very low | 1 | 0.06 | 0.09 |
| | | | low | 2 | 0.12 | |
| | | | Moderate | 3 | 0.18 | |
| | | | High | 4 | 0.28 | |
| | | | Very high | 5 | 0.37 | |
| Elevation (m) | 0.08 | | Very low | 1 | 0.06 | 0.09 |
| | | | low | 2 | 0.10 | |
| | | | Moderate | 3 | 0.21 | |
| | | | High | 4 | 0.27 | |
| | | | Very high | 5 | 0.36 | |
| Slope | 0.12 | | Very low | 1 | 0.06 | 0.08 |
| | | | low | 2 | 0.12 | |
| | | | Moderate | 3 | 0.22 | |
| | | | High | 4 | 0.26 | |
| | | | Very high | 5 | 0.35 | |
| Drainage | 0.05 | | Very Poor | 1 | 0.07 | 0.07 |
| | | | Poor | 2 | 0.12 | |
| | | | Moderate | 3 | 0.20 | |
| | | | High | 4 | 0.26 | |
| | | | Excessive | 5 | 0.35 | |
| Canal | 0.03 | | Very Poor | 1 | 0.07 | 0.07 |
| | | | Poor | 2 | 0.12 | |
| | | | Moderate | 3 | 0.20 | |
| | | | High | 4 | 0.26 | |
| | | | Excessive | 5 | 0.35 | |

| | | | | | |
|--------------------|------|---------------|---|------|------|
| Rainfall | 0.07 | Very low | 5 | 0.45 | 0.09 |
| | | low | 4 | 0.27 | |
| | | Moderate | 3 | 0.12 | |
| | | High | 2 | 0.09 | |
| | | Very high | 1 | 0.07 | |
| Evapotranspiration | 0.08 | Very low | 1 | 0.06 | 0.07 |
| | | low | 2 | 0.12 | |
| | | Moderate | 3 | 0.20 | |
| | | High | 4 | 0.26 | |
| | | Very high | 5 | 0.35 | |
| LULC | 0.13 | Crop land | 6 | 0.31 | 0.08 |
| | | Water body | 5 | 0.24 | |
| | | Barren land | 4 | 0.19 | |
| | | Scrub land | 3 | 0.13 | |
| | | Sandy area | 2 | 0.09 | |
| | | Built-up land | 1 | 0.05 | |
| | | | | | |
| LST | 0.05 | Very low | 1 | 0.06 | 0.07 |
| | | low | 2 | 0.10 | |
| | | Moderate | 3 | 0.16 | |
| | | High | 4 | 0.28 | |
| | | Very high | 5 | 0.39 | |

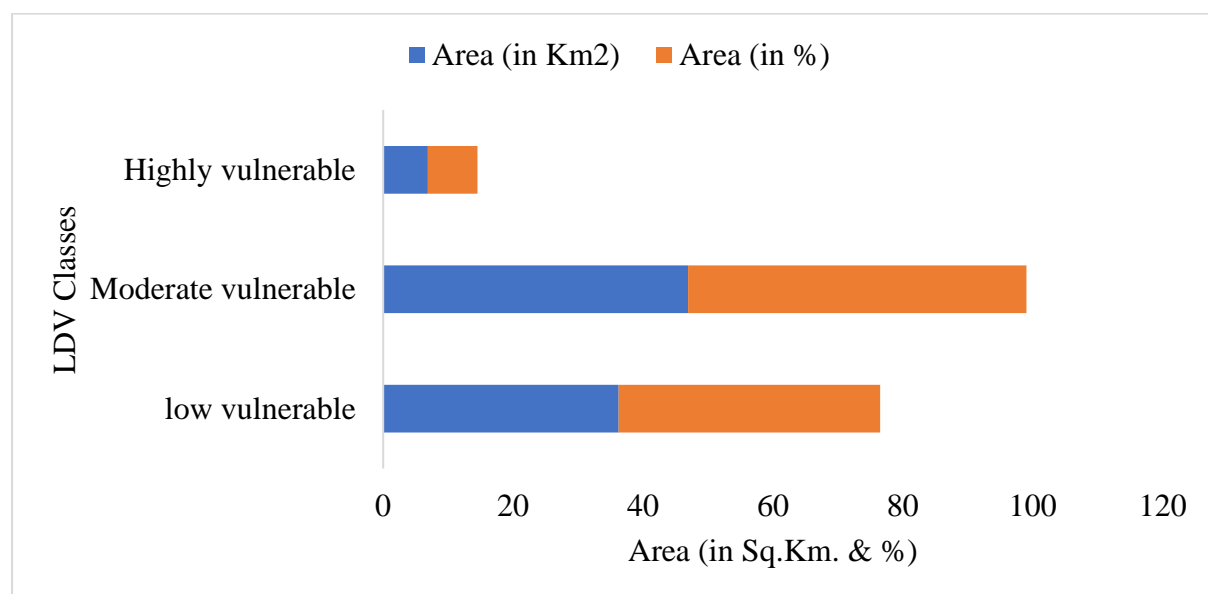


Figure 10 The area covered under different LDV classes

3.8. Validation of the results

For visual validation, LDVI classes in the study area were cross-referenced using high-resolution Google Earth as illustrated in Figure 11. The visual validation process involved assessing the LDVI classes: Highly vulnerable (Site 1), highly vulnerable (Site 2), Moderate vulnerable (Site 3), Moderate vulnerable (Site 4), Low vulnerable (Site 5), and Low vulnerable (Site 6), utilizing high-resolution image captured during the study time of the year 2018. The results of this validation clearly demonstrate a strong agreement between the observed land degradation characteristics in the Google Earth images of the selected areas and the output derived from the AHP- and GIS-based modeling conducted in the study.

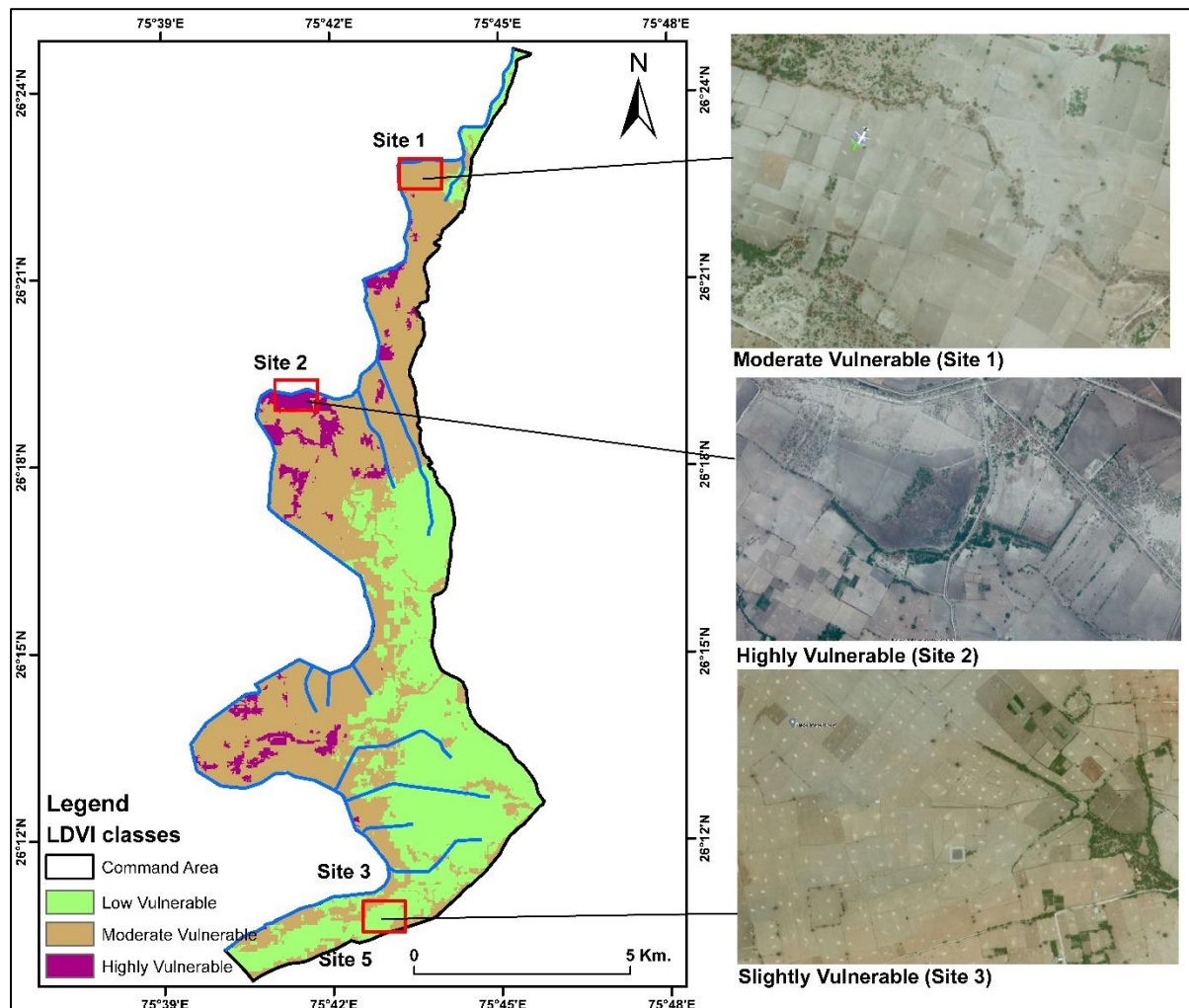


Figure 11 Validation of LDVI map from Google Earth image

Furthermore, the accuracy of the AHP models was assessed using the Receiver Operating Characteristic (ROC) curve and curve is depicted in Figure 12. The ROC curve, a common tool for accuracy assessment, plotted the true positive rate against the false positive rate. Site selection from Google Earth images helped test the performance of the AHP model in the study area. The ROC curve for the LD fields attained using the AHP method showed an Area under the Curve (AUC) value of 80.6%, with a standard error of 0.03 at a 5% significance level. This suggests that the AHP model produces reasonable and reliable results in predicting land degradation vulnerability fields in the study area.

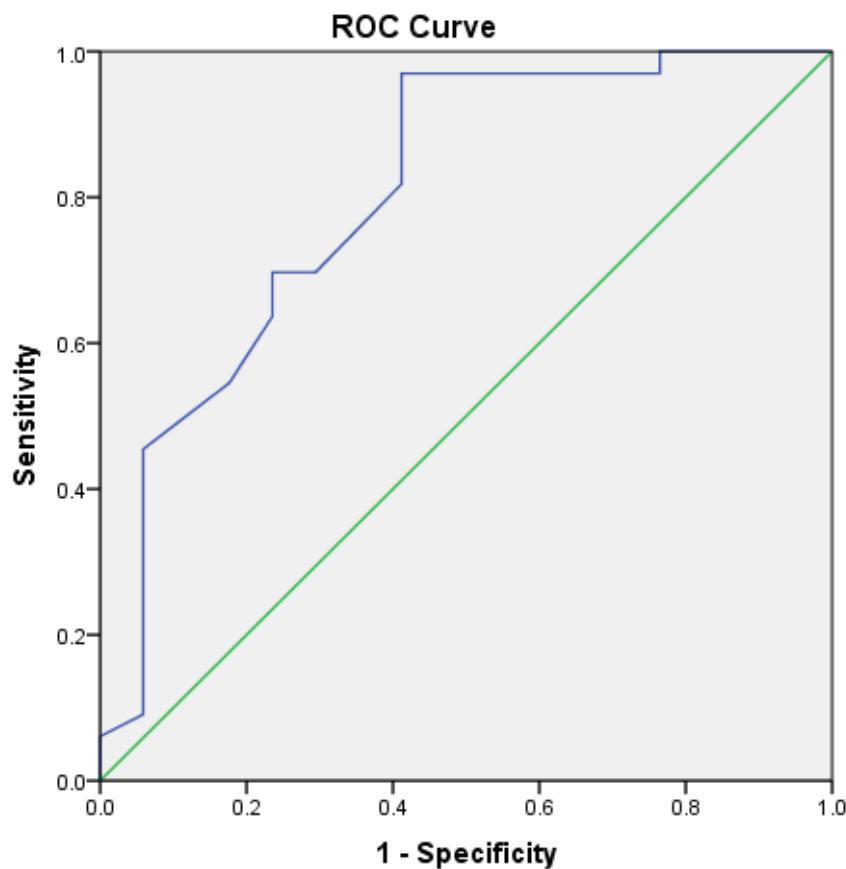


Figure 12 ROC curve of the LDV index attained using the AHP method

4. Conclusions

Land degradation, resulting from both human and anthropogenic activities, poses a significant challenge globally. This study investigates the use of geospatial technologies and the Analytic Hierarchy Process (AHP) to assess land degradation in the Mashī dam command area in India. Ten parameters, including electrical conductivity (EC), exchangeable sodium percentage (ESP), elevation, slope, drainage, canal system, rainfall, evapotranspiration, land use/land cover (LULC), and land surface temperature, were employed to evaluate land degradation. Moreover, the methodology applied in this study holds broader applicability and can be extended to arid and semi-arid regions, as well as other parts of India facing significant land degradation challenges. The insights gained from this research contribute to the understanding and potential mitigation of land degradation issues in various geographic contexts.

References

- [1] Abuzaid, A. S., Abdel Rahman, M. A., Fadl, M. E., & Scopa, A. (2021). Land degradation vulnerability mapping in a newly-reclaimed desert oasis in a hyper-arid agro-ecosystem using AHP and geospatial techniques. *Agronomy*, 11(7), 1426.
- [2] Ahmad, N., & Pandey, P. (2018). Assessment and monitoring of land degradation using geospatial technology in Bathinda district, Punjab, India. *Solid Earth*, 9(1), 75-90.
- [3] Ambarwulan, W., Nahib, I., Widiatmaka, W., Suryanta, J., Munajati, S. L., Suwarno, Y., ... & Sutrisno, D. (2021). Using geographic information systems and the analytical hierarchy process for delineating erosion-induced land degradation in the middle Citarum Sub-Watershed, Indonesia. *Frontiers in Environmental Science*, 9, 710570.

-
- [4] Basu, T., Das, A., Pham, Q. B., Al-Ansari, N., Linh, N. T. T., & Lagerwall, G. (2021). Development of an integrated peri-urban wetland degradation assessment approach for the Chatra Wetland in eastern India. *Scientific reports*, 11(1), 4470.
 - [5] Beinroth, F. H., Jones, J. W., Knapp, E. B., Papajorgji, P., & Luyten, J. (1998). Evaluation of land resources using crop models and a GIS. *Understanding options for agricultural production*, 293-311.
 - [6] Costantini, E. A., L'Abate, G., Faz Cano, A., Mermut, A., Arocena, J., & Ortiz Silla, R. (2009). A soil aridity index to assess desertification risk for Italy. *Land Degradation and Rehabilitation—Dryland Ecosystems. Advances in GeoEcology*, 40, 231-242.
 - [7] Crossland, M., Winowiecki, L. A., Pagella, T., Hadgu, K., & Sinclair, F. (2018). Implications of variation in local perception of degradation and restoration processes for implementing land degradation neutrality. *Environmental development*, 28, 42-54.
 - [8] Das, B., Desai, S., Daripa, A., Anand, G. C., Kumar, U., Khalkho, D., ... & Kumar, P. (2023). Land degradation vulnerability mapping in a west coast river basin of India using analytical hierarchy process combined machine learning models. *Environmental Science and Pollution Research*, 1-16.
 - [9] Gichenje, H., Pinto-Correia, T., & Godinho, S. (2019). An analysis of the drivers that affect greening and browning trends in the context of pursuing land degradation-neutrality. *Remote Sensing Applications: Society and Environment*, 15, 100251.
 - [10] Gomiero, T. (2016). Soil degradation, land scarcity and food security: Reviewing a complex challenge. *Sustainability*, 8(3), 281.
 - [11] Hossain, A., Krupnik, T. J., Timsina, J., Mahboob, M. G., Chaki, A. K., Farooq, M., ... & Hasanuzzaman, M. (2020). Agricultural land degradation: processes and problems undermining future food security. In *Environment, climate, plant and vegetation growth* (pp. 17-61). Cham: Springer International Publishing.
 - [12] Jaafari, A., Janizadeh, S., Abdo, H. G., Mafi-Gholami, D., & Adeli, B. (2022). Understanding land degradation induced by gully erosion from the perspective of different geoenvironmental factors. *Journal of Environmental Management*, 315, 115181.
 - [13] Kumar, P., & Sharma, P. K. (2020). Soil salinity and food security in India. *Frontiers in Sustainable Food Systems*, 4, 533781.
 - [14] Kundu, A., Dutta, D., Patel, N. R., Denis, D. M., & Chattoraj, K. K. (2021). Evaluation of socio-economic drought risk over Bundelkhand region of India using analytic hierarchy process (AHP) and geo-spatial techniques. *Journal of the Indian Society of Remote Sensing*, 49, 1365-1377.
 - [15] Lamat, R., Kumar, M., Kundu, A., & Lal, D. (2021). Forest fire risk mapping using analytical hierarchy process (AHP) and earth observation datasets: A case study in the mountainous terrain of Northeast India. *SN Applied Sciences*, 3(4), 425.
 - [16] Maji, B., & Lama, T. D. (2016). Improving productivity of vulnerable coastal soils under changing climate. *SATSA Mukhapatra-Annual Technical Issue*, 20, 46-52.
 - [17] Mashame, G., & Akinyemi, F. (2016). Towards a remote sensing based assessment of land susceptibility to degradation: Examining seasonal variation in land use-land cover for modelling land degradation in a semi-arid context. *ISPRS Annals of the Photogrammetry, Remote Sensing and Spatial Information Sciences*, 3, 137-144.
 - [18] Mohamed, E., Belal, A. A., Ali, R. R., Saleh, A., & Hendawy, E. A. (2019). Land degradation. The soils of Egypt, 159-174.
 - [19] Moharir, K. N., Pande, C. B., Gautam, V. K., Singh, S. K., & Rane, N. L. (2023). Integration of hydrogeological data, GIS and AHP techniques applied to delineate groundwater potential zones in sandstone, limestone and shales rocks of the Damoh district, (MP) central India. *Environmental research*, 228, 115832.
 - [20] Morgado, R. G., Loureiro, S., & González-Alcaraz, M. N. (2018). Changes in soil ecosystem structure and functions due to soil contamination. In *Soil pollution* (pp. 59-87). Academic Press.
 - [21] Mzuri, R. T., Mustafa, Y. T., & Omar, A. A. (2022). Land degradation assessment using AHP and GIS-based modelling in Duhok District, Kurdistan Region, Iraq. *Geocarto International*, 37(25), 7908-7926.

- [22] Perri, S., Molini, A., Hedin, L. O., & Porporato, A. (2022). Contrasting effects of aridity and seasonality on global salinization. *Nature Geoscience*, 15(5), 375-381.
- [23] Pessoa, L. G., Freire, M. B. D. S., Green, C. H., Miranda, M. F., de A Filho, J. C., & Pessoa, W. R. (2022). Assessment of soil salinity status under different land-use conditions in the semiarid region of Northeastern Brazil. *Ecological Indicators*, 141, 109139.
- [24] Pravalie, R., Patriche, C., Borrelli, P., Panagos, P., Roşca, B., Dumitraşcu, M., ... & Bandoc, G. (2021). Arable lands under the pressure of multiple land degradation processes. A global perspective. *Environmental Research*, 194, 110697.
- [25] Roy, P., Pal, S. C., Chakraborty, R., Saha, A., & Chowdhuri, I. (2023). A systematic review on climate change and geo-environmental factors induced land degradation: Processes, policy-practice gap and its management strategies. *Geological Journal*, 58(9), 3487-3514.
- [26] Saaty, T. (1980, November). The analytic hierarchy process (AHP) for decision making. In Kobe, Japan (Vol. 1, p. 69).
- [27] Sandeep, P., Reddy, G. O., Jegan kumar, R., & Arun Kumar, K. C. (2021). Modeling and assessment of land degradation vulnerability in semi-arid ecosystem of Southern India using temporal satellite data, AHP and GIS. *Environmental Modeling & Assessment*, 26, 143-154.
- [28] Shao, W., Zhang, Z., Guan, Q., Yan, Y., & Zhang, J. (2024). Comprehensive assessment of land degradation in the arid and semiarid area based on the optimal land degradation index model. *Catena*, 234, 107563.
- [29] Sinshaw, B. G., Belete, A. M., Tefera, A. K., Dessie, A. B., Bizuneh, B. B., Alem, H. T., ... & Moges, M. A. (2021). Prioritization of potential soil erosion susceptibility region using fuzzy logic and analytical hierarchy process, upper Blue Nile Basin, Ethiopia. *Water-Energy Nexus*, 4, 10-24.
- [30] Smith, P., Ashmore, M. R., Black, H. I., Burgess, P. J., Evans, C. D., Quine, T. A., ... & Orr, H. G. (2013). The role of ecosystems and their management in regulating climate, and soil, water and air quality. *Journal of Applied Ecology*, 50(4), 812-829.
- [31] Thiam, S., Villamor, G. B., Faye, L. C., Sène, J. H. B., Diwediga, B., & Kyei-Baffour, N. (2021). Monitoring land use and soil salinity changes in coastal landscape: A case study from Senegal. *Environmental Monitoring and Assessment*, 193, 1-18.
- [32] Xie, H., Zhang, Y., Wu, Z., & Lv, T. (2020). A bibliometric analysis on land degradation: Current status, development, and future directions. *Land*, 9(1), 28.
- [33] Yousefi, H., Motlagh, S. G., & Montazeri, M. (2022). Multi-Criteria Decision-Making System for Wind Farm Site-Selection Using Geographic Information System (GIS): Case Study of Semnan Province, Iran. *Sustainability*, 14(13), 7640.